

# Development of analysis tools for self-rectifying impulse turbines for OWC systems

The paper presents the development of Performance Analysis Tools for Impulse-turbines for Oscillating water column wave energy converters, PATIOS. PATIOS applies the experimental correlations for axial turbomachines to self-rectifying impulse turbine and, with limited computational resources, provides prompt results as well as quantitative and qualitative analysis of the losses. Models and correlations for an OWC system with self-rectifying impulse turbine are presented and analyzed; the whole set was implemented in Matlab-Simulink environment. CFD simulations have been run to validate the results. PATIOS has been used for a wide-range sensitivity analysis, identifying the most relevant design variables and comparing the results with the experimental ones, available in the literature.

DOI: 10.12910/EAI2015-037

■ G. Cafaggi, G. Manfrida, L. Cappiotti

## Introduction

The harvesting of offshore renewable energies is an emerging topic in the scientific and technical field. Among other renewable energies, the conversion of wave energy [1, 2, 3] into a usable form has stimulated many researchers to develop Wave Energy Converters (WEC). At present there are thousands of patents in this sector. However, no one of these WECs has reached a commercial level and just few have reached a post-demonstration phase [4].

An Oscillating Water Column (OWC) is a WEC that comprises a partly submerged structure, open below the water surface, inside which a volume of air is trapped; the incident waves produce the oscillating motion of the internal free surface, making the air flow through a turbine that drives an electrical generator.

Some of the characteristics that make OWC systems promising WECs are their simplicity and absence of moving parts, except for the turbine. In the majority of works, the turbine is treated as a simplified linear system, and when this is not the case the design is mainly made by means of experimental campaigns or CFD simulations.

Recent development in the ongoing research on OWC systems [5, 6] seems to point out that the self-rectifying impulse turbine will be a better alternative to the traditionally used Wells turbine.

This paper presents the development of PATIOS (Performance Analysis Tools for Impulse-turbines for OWC Systems): a suite of tools meant to help and quicken the study of OWC systems using fixed-guide vane, self-rectifying impulse turbines (Fig. 1), intended for the preliminary analysis of OWC systems in different locations and sea climates.

PATIOS proposes to apply experimental correlations of turbomachines commonly used in other fields as the guidelines for system design and analysis. The main advantage of this approach

■ Contact person: Giovanni Cafaggi  
giovanni.cafaggi@gmail.com

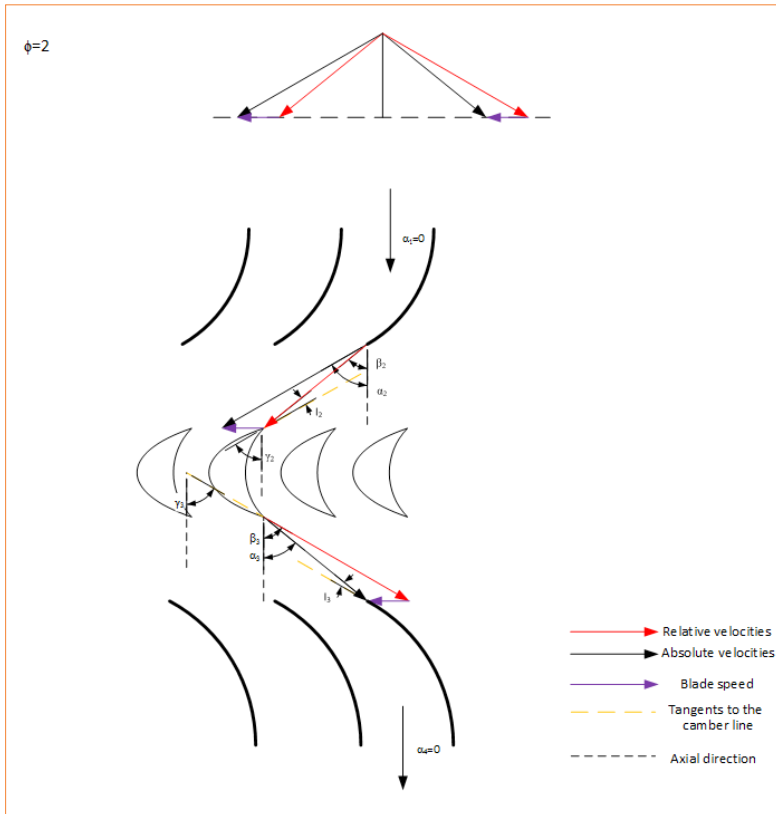


**FIGURE 1** Fixed-guide vane, impulse turbine triangle of velocities and geometry at mean radius

is a major reduction of time and resources needed (either economical or computational), with the possibility of examining and comparing a large number of different options. Moreover, a second advantage is that the turbine losses analysis obtained is not only quantitative, but also qualitative, since the correlations divide the losses in each blade row into different categories. Lastly, it is possible to couple completely the simulation of the caisson and of the turbine. The drawback is that since the experimental correlations are designed for the gas turbines from other fields of energy conversion their validation for the present objective is needed, possibly by detailed experimental measurements; an alternative – presented in this work – is to apply CFD calculations to this purpose.

## Turbine model

The examined system presents some peculiarities from a turbomachinery point of view: the fact that the turbine is operating with an alternating flow leads to the need for a symmetric geometry: thus, while the Inlet Guide Vane (IGV) is an accelerating row, the Outlet Guide Vane (OGV) is a diffusive one (Fig. 1). This also leads to the fact that the angles of incidence on the rotor and on the OGV blades are intrinsically remarkable. The non-dimensional variables used to characterize impulse turbines in OWC systems are the flow coefficient  $\phi$  (Eq. 2), the torque coefficient  $C_T$  (Eq. 3), and the input coefficient  $C_A$  (Eq. 4). These coefficients represent the axial velocity, the shaft torque and the power available for the turbine, respectively.

$$\eta = \frac{T\omega}{\Delta p \dot{V}} = \frac{C_T}{C_A \phi} \quad (1)$$

$$\phi = \frac{c_x}{u_m} \quad (2)$$

$$C_T = \frac{2T}{\rho(c_x^2 + u_m^2) H l_r z r_m} \quad (3)$$

$$C_A = \frac{2\Delta p \dot{V}}{\rho(c_x^2 + u_m^2) H l_r z c_x} \quad (4)$$

$$P = L_{sp} \dot{m} = T\omega \quad (5)$$

These parameters are directly related to the efficiency  $\eta$  (Eq. 1), and through the rotational speed  $\omega$ , the flow rate and the geometry of the turbine to the mechanical power available at the shaft  $P$  (Eq. 5) and to the total pressure drop across the turbine,  $\Delta p$ . The fundamental Euler equation for turbomachinery relates the specific work and thus the shaft power to the velocity triangles of the rotor stage. A number of experimental correlations to determine the

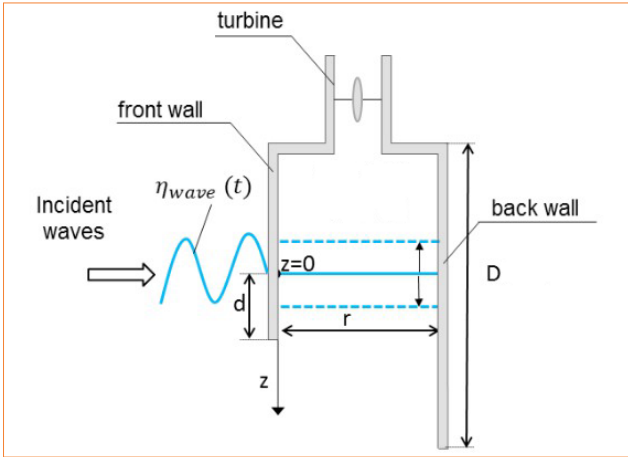


FIGURE 2 OWC system scheme

deviation of the flow, as well as the total pressure loss, can be found in the literature for turbine [14, 15, 16, 17] and compressor [13, 18] cascade rows. By applying the correlations, it is possible to calculate the loss coefficient and the resulting  $\Delta p$ ; by removing the kinetic component, the static pressure drop  $\Delta p_s$  is obtained. This calculation can be repeated for different flow rates (covering the full off-design operating range, within the boundaries connected with the specific correlation used), determining the expected characteristic curve of the turbine,  $\Delta p_s = f(\dot{m})$ .

### Simplified caisson model

While the rotational speed and the geometry can be chosen at will, the axial velocity is dependent on the caisson characteristics and on the features of the incoming wave, which is the real input for an OWC system. One of the possible methods to model the caisson is the weightless piston model (Fig. 2). Considering the mass of water adjacent to the free surface inside the caisson as a rigid body, and applying the Newton's second law, it is possible to obtain its equation of motion, thus giving the height of the water column (Eq. 6, 7, 8, 9 and 10).

$$m\ddot{z} = f_e + f_{rad} + f_{hstat} - f_p \quad (6)$$

$$f_e = A_c \rho g H \cos(\omega t + \varphi) \frac{\cosh k(h-d)}{\cosh(kh)} \quad (7)$$

$$f_{rad} = m_a \ddot{z} + B_r \dot{z} \quad (8)$$

$$f_{hstat} = A_c \rho g [d - (z - h_p)] - A_c \rho g h_p = A_c \rho g (d - z) \quad (9)$$

$$f_p = A_c \Delta p_s \quad (10)$$

The free surface motion is then linked to the mass flow through the turbine by the equation (Eq. 11):

$$\dot{m}_t = \frac{-d(\rho_{air} V)}{dt} = \rho_{air} A_c \frac{dz}{dt} - \frac{(v_0 - z A_c) dp}{c^2} \frac{dp}{dt} \quad (11)$$

### Coupling caisson and turbine

Using the experimental correlation method mentioned above and fixing the rotational speed and geometry, it is possible to consider the  $\Delta p_s = f(c_x)$  that together with equations 6 and 11 forms a system of differential equations, which can be solved by numerical methods once the geometry of the system and the fundamental features of the incoming wave are given.

In the turbine performance calculation, a dynamic stall model can also be implemented; in fact, it is well-known that airfoils can resist in dynamic conditions without profile stall to very large angles of attack. The dynamic stall model developed by Strickland *et al.* [7] (eq. 12, 13, 14) enables to calculate an equivalent angle of attack  $\alpha_m$  for each row. This angle is then the one used to find the pressure losses.

$$\alpha_m = \alpha - \gamma K_1 S_{\dot{\alpha}} \sqrt{\left(\frac{c\dot{\alpha}}{2W}\right)} \quad (12)$$

$$K_1 = 0,75 + 0,25 S_{\dot{\alpha}} \quad (13)$$

$$\gamma = 1,4 - 6(0,06 - t/C) \quad (14)$$

## Development of modeling tools and examples of results

The above theory and equations have been coded into Matlab language to provide an easy-to-modify, fast, and reliable system simulator. Two are the main tools developed in this way.

The first tool implements only the turbine performance calculation theory for stationary flow: given geometry and design axial velocity, it calculates the working curves of the turbine.

The second comprehends the caisson equations and performs a wave to shaft simulation, given system geometry, incoming wave shape and initial conditions.

### Turbine stationary simulator

After evaluating and testing the most popular correlations describing the performance of axial turbines, the set which has been found best suited and, consequently, implemented for simulations includes the modified Ainley-Mathieson and Carter-Hughes correlations for rotor and IGV rows, and Howell's correlation for the diffusive row [8].

A series of simulations has been carried out using this tool on turbines of different sizes (with blade angles

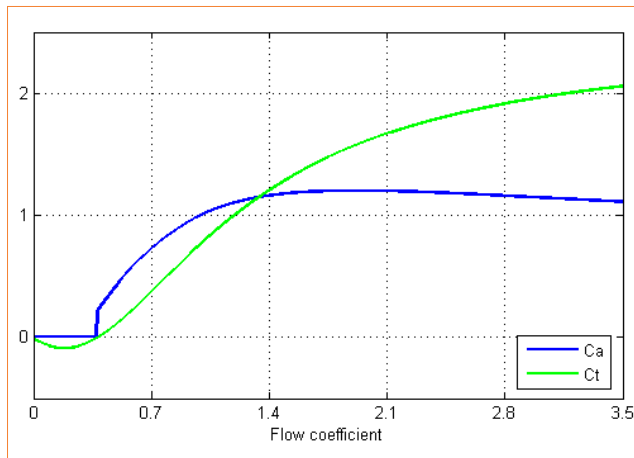


**FIGURE 3** Input and torque coefficient for varying flow coefficients

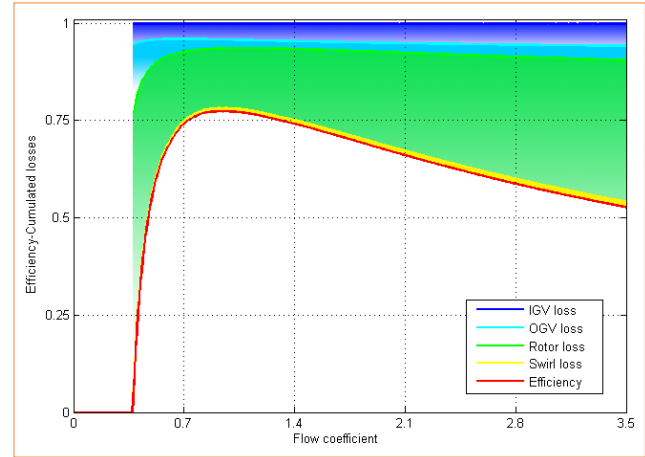


**FIGURE 4** Efficiency and losses in each row

suggested by Setoguchi *et al.* [9] and an outer radius of 0.15 m, 0.5 m and 1.3 m) for a wide range of flow rates. The typical trends of the non-dimensional coefficients  $C_T$  and  $C_A$  can be seen in Figure 3. The input coefficient  $C_A$  is artificially set to zero when the machine is not working properly, that is, when the power generated is negative (in this case, the experimental correlations are clearly not valid anymore).

One of the advantages of this approach is that the losses are found separately for each blade row (Fig.

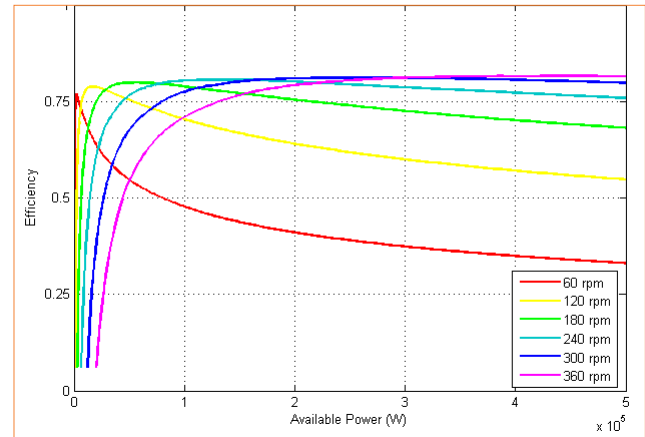


**FIGURE 5** Turbine efficiency against available power for different rotational speeds

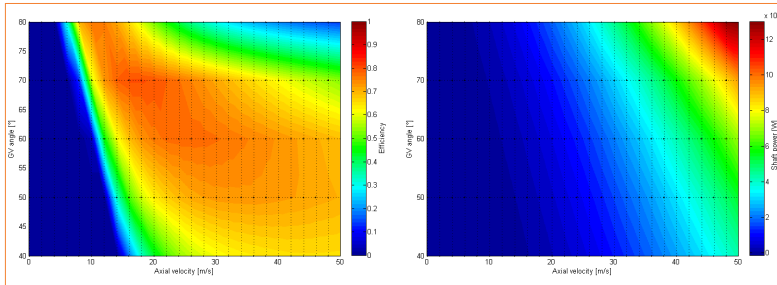


**FIGURE 6** Efficiency and shaft power mapping for varying GV blade angles and axial velocity

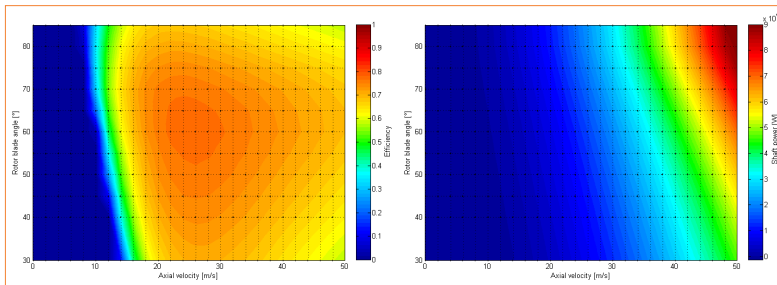


**FIGURE 7** Efficiency and shaft power mapping for varying rotor blade angles and axial velocity

4); moreover, in each blade row, depending on the correlation used, the losses are internally subdivided as profile, secondary, incidence and annulus losses. The trends for non-dimensional coefficients and efficiency are in line with experimental studies found in the literature.

Since the tool developed is of quick use (compared to CFD and experimental methods), during the simulation campaign it is convenient to run a sensitivity analysis on parameters like rotor speed, hub-to-tip ratio, stator and rotor blade angles. This analysis was mainly aimed at obtaining data to compare with the literature sources and not at optimizing a certain geometry.

The first sensitivity analysis was run varying the rotor speed of each turbine, but maintaining the geometry fixed: in Figure 5 one of the resulting graphs can be observed. The efficiency is given as a function of the available power,  $P_{av}$ , so that the graph can be compared with the one given by Thakker *et al.* [10], which reports

different numerical values (also due to the dimensional nature of the available power variable), but identical trends.

In another set of simulations the effect of changing the outlet blade angle of the IGV (and the inlet blade angle of the OGV in order to keep the geometry symmetrical) was studied. As can be seen in Figure 6, the best efficiency on a wide range of axial velocities is obtained for 60° in accordance with the experimental studies found in the literature [9]. An interesting fact is that the shaft power is always higher for the 80° blade angle; this is explained observing both figures and remembering the efficiency and shaft power definitions (eq. 1 and 5): axial velocity and flow rate are proportional, since the inlet area is constant, therefore the pressure drop across the turbine results higher for lower efficiency and higher shaft power.

In Figure 7 the same kind of mapping can be observed changing the inlet

and outlet (symmetrical) blade angles of the rotor. The variations of efficiency and shaft power are not as pronounced as in the case of the guide-vane angles, but present a clear optimum point at 60°, with highest efficiency on the widest range of axial velocity. The differences with the mapping obtained changing GV angles seem to point out that rotor angles could be tuned with some flexibility without compromising the performance of the system. To have a partial confirmation of the results obtained with this method, a series of CFD simulations on the rotor row have been carried out for different axial velocities at turbine inlet and a comparison of the losses has been made.

An example of the results is shown in Figure 8; the loss coefficients  $\xi$  calculated from the total pressure field are compared in Table 1 with the values calculated by the model; it can be seen that the model provides reasonable results, with better accuracy for higher flow coefficients.

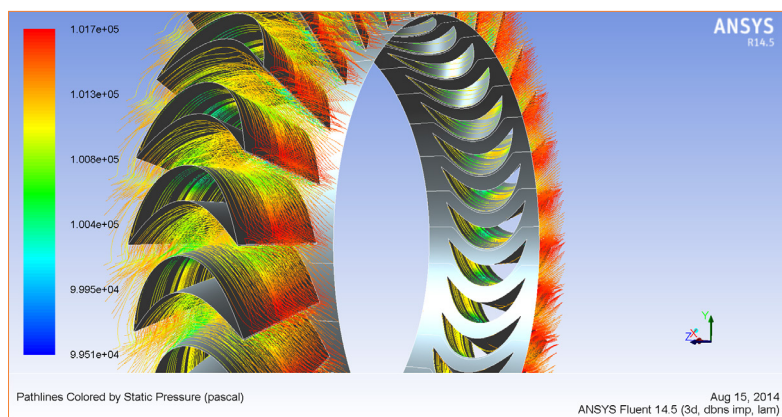


**FIGURE 8** Streamlines through the rotor, depicting static pressure and flow direction

$\varphi$	$\xi$ CFD	$\xi$ Model
1,5	0,47	0,33
3,0	0,43	0,43
4,5	0,52	0,46
6,0	0,56	0,46
7,5	0,56	0,45

**TABLE 1** Comparison of loss coefficient obtained using CFD and PATIOS (rotor)

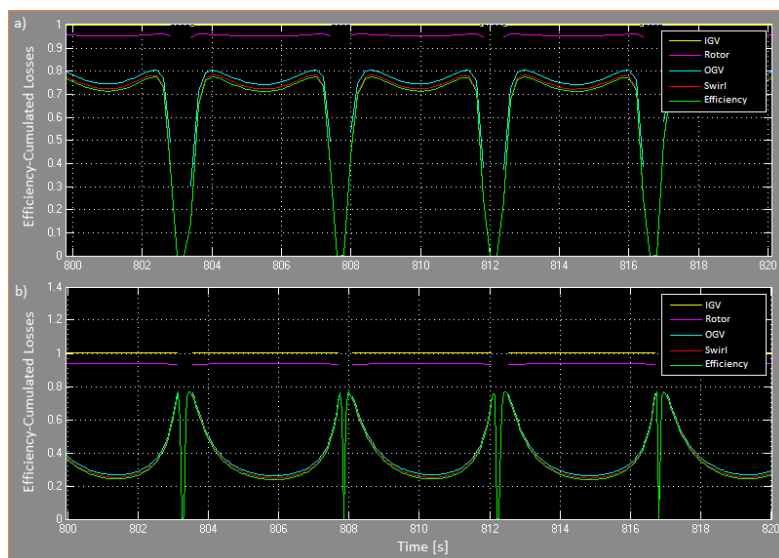


**FIGURE 9** Efficiency and cumulative losses in each row for turbines with suitable (a) and not (b) geometries

## Wave-to-shaft simulator

The wave-to-shaft simulator was developed in Simulink. It uses the numerical methods available in this environment for the solution in the time domain of the dynamic system differential equations coupled with the off-design turbine performance model. The caisson model implemented in the simulator is a modified weightless piston model [8]. The main inputs of the simulator are the geometry of the system, the incoming wave shape (as a sum of sinusoidal components) and the fixed rotational speed of the turbine. The main outputs are the instantaneous values of shaft power, pressure drop across the turbine and flow rate. Other variables extracted during the development process to observe the behavior of the system are the free surface level inside the caisson and its speed and acceleration, the pressure at the base of the caisson, and the axial velocity at the turbine inlet. A post-processing routine has been implemented to obtain efficiencies, losses, averaged values of all relevant parameters and graphs directly from the simulator. The efficiency and losses are calculated for the turbine in the same way as in the stationary code (efficiency of Eq. 1 and losses divided by row and cause). In Figure 9 two relevant cases are shown, depicting the efficiency and losses of two different turbines applied to the same caisson with the same incoming wave. The first turbine has values of rotational speed and stator blade angles optimized for the incoming wave. The second turbine reaches its peak efficiency just after the inversion of the flow, thus it would result better

Period [s]	Amplitude [m]	Average Shaft Power (kW)		Difference	
		with Dynamic stall	Simplified	Absolute	%
3	0,5	-0,07	-0,071	0,001	-1,43
4,5	0,75	0,188	0,187	0,001	0,53
5,5	1,1	19,16	19,18	-0,020	-0,10
6	1,5	54,6	54,5	0,100	0,18
7,5	2,25	77,2	76,9	0,300	0,39
9	3	85	85,1	-0,100	-0,12
Overall	-	236,08	235,80	0,282	0,12

**TABLE 2** Comparison of shaft power obtained with and without the dynamic stall model

suiting for lower axial velocities, that is, for incoming waves of smaller amplitude or longer period, but its performance deteriorates at higher flow rates where the energy that could be extracted is maximum.

A series of simulations have been carried out using sinusoidal waves with amplitude and length typical of the Tyrrhenian Sea [11]. The goal of the first set of simulation was to validate the relevance of the dynamic stall model. In practice, dynamic stall is proportional to the change in angle of attack, that is most evident for this highly unsteady flow application in proximity of the change of airflow direction. This zone is also the one in which the power available and, consequently, the shaft power are close to their minimum values, so it was reasonable to expect that the impact of the dynamic stall effect would be negligible. This was the case, in fact the simulations led to the results shown in Table 2, which presents the difference in the estimated shaft power for the two simulators. This conclusion however applies only to the sea conditions here considered (northern Tyrrhenian Sea), therefore for different locations the comparison should be made again, including the specific frequency and amplitude values.

The wave-to-shaft simulator has also been used to observe the effect of variation of coefficient  $B_r$  in the caisson model since, according to the studies from which the values used are taken [12], it is the one with the largest degree of uncertainty [8]. Lastly the model has been used to map the average efficiency of the system for the range of incoming waves already described. Some of the results obtained from this campaign are visible in Figure 10. It can be observed that the efficiency of the turbine is relatively flat compared to the one of the caisson. It seems, in fact, that the performance of the latter is closely related to the frequency of the incoming wave and reaches its peak for a certain

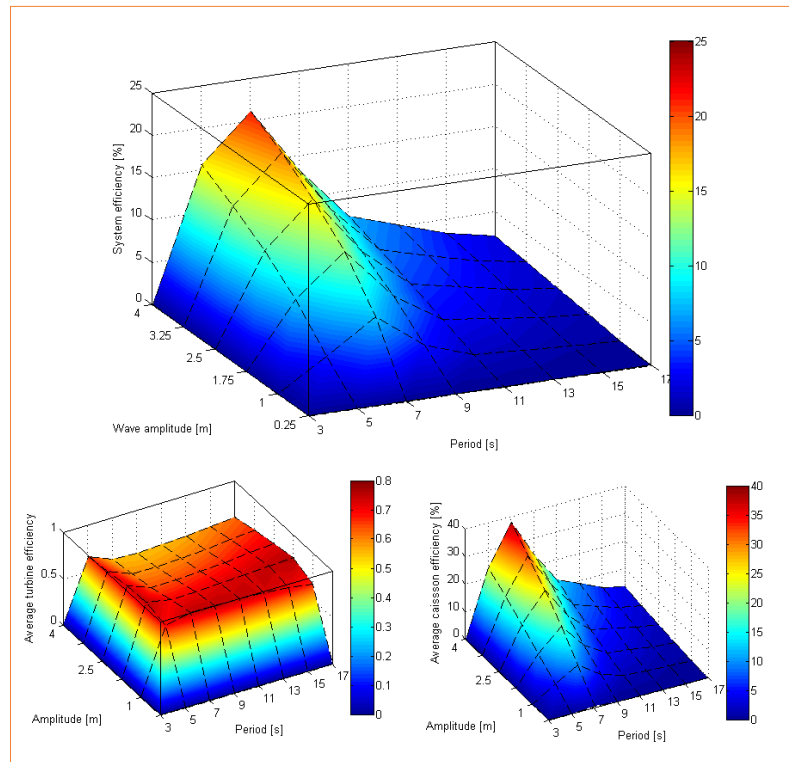


**FIGURE 10** Average system, turbine and caisson efficiencies for varying incident waves

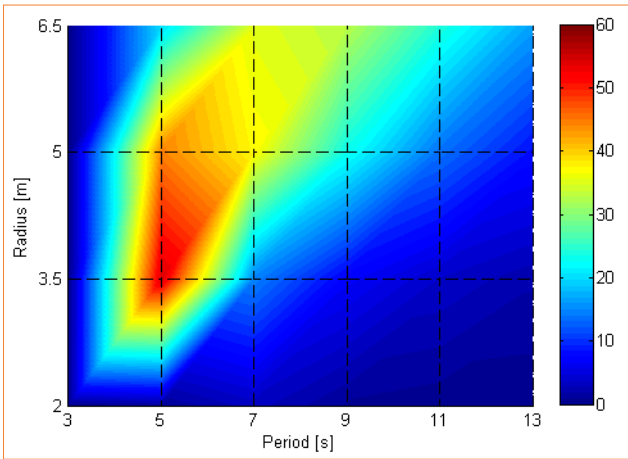


**FIGURE 11** Average system efficiency mapping for varying incoming wave period and caisson geometry

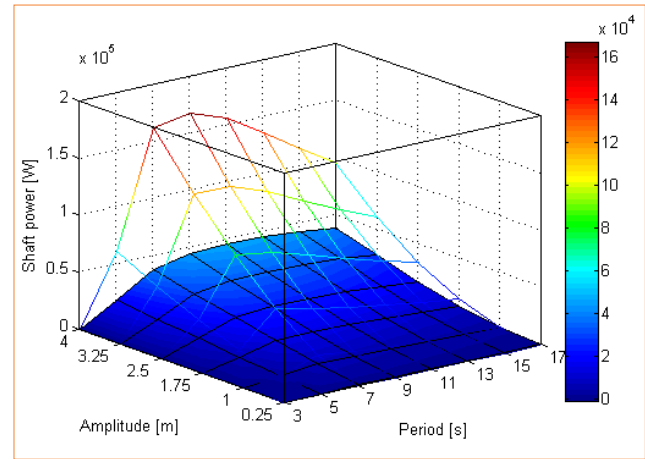


**FIGURE 12** Comparison of shaft power of turbine with suitable geometry (netting) and not (surface)

frequency independently from the wave amplitude. A further study revealed that this frequency is closely related with the caisson dimensions (Fig. 11). The same simulations have been run using turbines

with different geometries and the results have been compared. The parameter used for this comparison was the shaft power, since from an economic point of view this is the parameter directly related with profit when considering null the marginal costs, and the O&M and capital costs independent from the turbine geometry. The example in Figure 12 shows a situation in which the device represented by the netting is clearly more suited than the one represented by the surface on the whole range of incoming waves.

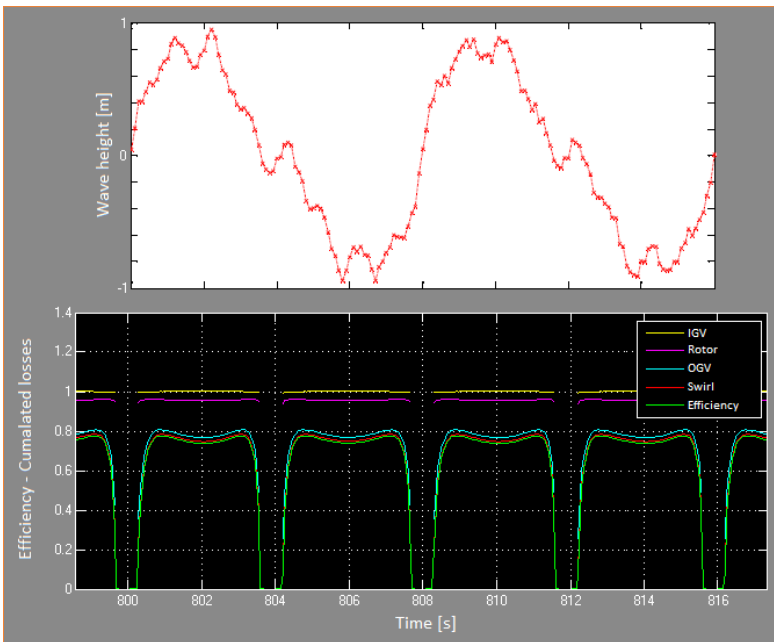


**FIGURE 13** Irregular incoming wave shape (over) and resulting efficiency and losses (below)

Simulations have also been run with irregular waves (Fig. 13), but the results show that higher frequency components are subject to a high damping – at first through the coefficient  $\Gamma$ , which is calculated independently for each wave component, then both in the calculation of the free surface motion and of the turbine inlet velocity. This was confirmed by the negligible magnitude of higher frequency components in the efficiency and loss curves (Fig. 13).



## Conclusions

In order to develop PATIOS (Performance Analysis Tools for Impulse-turbines for OWC Systems), a set of experimental correlations for axial turbines has been applied to self-rectifying impulse designs. The relevance of the effects of profile dynamic stall was assessed, a simple unsteady model for the caisson has been coupled to the turbine correlations under off-design; the whole set has been implemented in a Matlab-Simulink environment. A simulation campaign has been carried out using these tools to provide data comparable with the technical literature, and to perform a sensitivity analysis on the main design parameters. The comparison with the literature and with a set of CFD results for the rotor blade row shows an agreement in the trends for characteristic curves and efficiencies in all cases; however, the off-design performance of the simulated turbine results optimistic with respect to experiments or CFD. This could be due to several reasons: the experimental correlations were not originally intended for this kind of application, therefore it is possible that the blade profiles they refer to are more optimized than those actually used for OWC impulse turbines; moreover, the calculated losses are not influenced by the distance among the blade rows, while in the literature [9] this effect is considered relevant enough to be studied on its own. Direct or model testing are clearly needed to improve the accuracy of the correlations. The caisson model would also need more experimental data on different caisson sizes and shapes for the estimate of coefficients  $B_r$  and  $m_a$ . At the present stage, the tools developed seem well suited to conduct quick preliminary analyses and comparison of different OWC systems. Future development of this project includes the implementation of electrical components in the simulator and a study of the system inertia, in order to simulate also the starting characteristics of the system; after tuning of the model, it should be possible to consider long-term simulations with real sea conditions, and to ascertain the possible benefits of operation with multiple, or variable rotational speeds and with a seasonal variable geometry of the caisson.

## List of variables

$A_c$	horizontal caisson area
$B_r$	experimental radiation damping coefficient
$C_A$	Input coefficient
$C_T$	torque coefficient
$c_x$	axial velocity
$d$	OWC front wall draught
$g$	gravity acceleration
$H_i$	$i^{\text{th}}$ incident wave component amplitude
$h_p$	height of the rigid water body considered
$H_r$	rotor blades height
$l_r$	chord length of rotor blade
$m$	mass of water considered as rigid body
$m_a$	experimental added mass coefficient
$\dot{m}_t$	air mass flow through the turbine
$S_{\dot{\alpha}}$	sign of $\dot{\alpha}$
$t_r$	maximum blade thickness
$t$	time
$T$	Torque
$P$	shaft power
$U_m$	$\omega r_m$ = circumferential velocity at $r_m$
$\dot{V}$	flow rate
$V_c$	air volume inside the caisson
$V_0$	air volume inside the caisson when $z=0$
$w$	relative velocity at rotor inlet
$z$	height of the free surface inside the caisson
$z_r$	number of rotor blades
$\alpha$	angle of attack
$\alpha_m$	equivalent angle of attack
$\Gamma_i$	$i^{\text{th}}$ incident wave component depth damping factor
$\Delta p$	total pressure difference across the turbine
$\Delta p_s$	static pressure difference across the turbine
$\xi$	total pressure loss coefficient
$\phi_i$	$i^{\text{th}}$ incident wave component phase
$\Phi$	flow coefficient
$\rho$	water density
$\rho_a$	air density
$\omega$	rotational speed
$\omega_i$	$i^{\text{th}}$ incident wave component frequency

Giovanni Cafaggi, Giampaolo Manfrida, Lorenzo Cappiatti  
University of Florence, Italy

- [1] A. Clement, P. McCullen, A. Falcão, A. Fiorentino, F. Gardner, K. Hammarlund, G. Lemonis, T. Lewis, K. Nielsen, S. Petroncini, M.T. Pontes, P. Schild, B.O. Sjöström, H.C. Sørensen, T. Thorpe, Wave energy in Europe: current status and perspectives, in *Renewable and sustainable energy reviews*, 6(5), pp. 405-431, 2002.
- [2] D. Vicinanza, L. Cappiotti, V. Ferrante, P. Contestabile, Estimation of the wave energy in the Italian shore, in *Journal of Coastal Research*, 64(12), pp. 613-617, 2011.
- [3] V. Vannucchi, L. Cappiotti, Wave Energy Estimation in Four Italian Nearshore Areas, from *ASME 2013 32<sup>nd</sup> International Conference on Ocean, Offshore and Arctic Engineering*, Volume 8: Ocean Renewable Energy Nantes, France, June 9–14, 2013, ISBN: 978-0-7918-5542-3, doi:10.1115/OMAE2013-10183.
- [4] A.F.O. Falcão, Wave energy utilization: A review of the technologies, in *Renewable and Sustainable Energy Reviews*, 14(3), pp. 899-918, 2010.
- [5] A.F.O. Falcão, L.M.C. Gato, E.P.A.S. Nunes, A novel radial self-rectifying air turbine for use in wave energy converters, in *Renewable Energy*, 53, pp.159-164, 2013.
- [6] T. Setoguchi, M. Takao, Current status of self rectifying air turbines for wave energy conversion, in *Energy Conversion and Management*, 47, pp. 2382–2396, 2006.
- [7] I. Paraschivoiu, *Wind Turbine Design*, Polytechnic International Press, Montreal, 2002.
- [8] G. Cafaggi, Development of analysis tools for self-rectifying impulse turbines for OWC systems, Master Thesis, Università degli Studi di Firenze, 2014.
- [9] T. Setoguchi, S. Santhakumar, H. Maeda, M. Takao, K. Kaneko, A review of impulse turbines for wave energy conversion, in *Renewable Energy*, 23, pp. 261–292, 2001.
- [10] A. Thakker, F. Hourigan, Modeling and scaling of the impulse turbine for wave power applications, in *Renewable Energies*, 29, pp.305-317, 2004.
- [11] V. Vannucchi, Wave Energy harvesting in the Mediterranean Sea, Tesi di dottorato, Università degli Studi di Firenze, Dottorato di ricerca in Ingegneria Civile e Ambientale, Ciclo XXV, 2013.
- [12] I. Simonetti, L. Cappiotti, G. Manfrida, H. Matthies, H. Oumeraci, State of the art review on analytical and numerical modelling for Oscillating Water Columns Wave Energy Converter Technology, internal report n° 2 (2013), Department of Civil and Environmental Engineering, Università degli Studi di Firenze, 2013.
- [13] S.L. Dixon, *Fluid Mechanics and Thermodynamics of Turbomachinery*, Fifth edition. Elsevier (Ed.), ISBN 978-0-7506-7870-4, 1998.
- [14] J.H. Horlock, *Axial Flow Turbines*, Butterworths (Ed.), London, 1966.
- [15] J. Dunham, P. Came, Improvements to Ainley-Mathieson method of turbine performance prediction, in *Trans. Am. Soc. Mech. Engrs.*, Series A, 92, 1970.
- [16] S.C. Kacker, U. Okapuu, A Mean Line Prediction Method for Axial Flow Turbine Efficiency, in *Journal of Engineering for Power*, vol. 104(1), pp. 111-119, 1982.
- [17] S.H. Moustapha, S.C. Kacker, B. Tremblay, An Improved Incidence Losses Prediction Method for Turbine Airfoils, in *ASME J. Turbomach.*, 112, pp. 267–276, 1990.
- [18] A.R. Howell, Design of axial compressors, in *Proc. Instn. Mech. Engrs.*, 153, 1945.